Differential Pathlength Spectroscopy for the Quantitation of Optical Properties of Gold Nanoparticles

Constantin Ungureanu,[†] Arjen Amelink,[‡,*] Raja G. Rayavarapu,[†] Henricus J. C. M. Sterenborg,[‡] Srirang Manohar,[†,*] and Ton G. van Leeuwen[†,§]

[†]Biomedical Photonic Imaging Group, MIRA Institute for Biomedical Technology and Technical Medicine, Faculty of Science and Technology, University of Twente, P.O. Box 217, 7500 AE Enschede, The Netherlands, [‡]Center for Optical Diagnostics and Therapy, Department of Radiation Oncology, Erasmus Medical Center, P.O. Box 2040, 3000 CA Rotterdam, The Netherlands, and [§]Academic Medical Center, Biomedical Engineering and Physics, University of Amsterdam, P.O. Box 22700, NL-1100 DE Amsterdam, The Netherlands

ABSTRACT An accurate estimation of optical absorption coefficient (μ_{abs}) and scattering coefficient (μ_{sca}) is important in characterizing nanoparticles for identifying or optimizing applications such as photothermal therapy and photoacoustic imaging. In this exciting period where several fascinating methods have been unveiled for the synthesis of various nanoparticles, the field is still lacking in the availability of efficient characterization methods. We introduce an accurate and simple methodology to optically characterize nanoparticles which could fill the gap. This is based on differential pathlength spectroscopy (DPS), a dual optical fiber approach, originally developed to detect cancer endoscopically by measuring the optical properties of tissue in small interrogation volumes. We expand its use to nanoparticles in a method that allows us to resolve the effects of μ_{abs} and μ_{sca} in the extinction coefficient of low concentration samples. We outline the measurement protocol using the DPS system and describe the analysis of the data taking additional inputs from electron microscopy and discrete dipole approximation (DDA) simulations. The DPS signal from the sample is first translated into the backscattering coefficient using a calibration constant. Further, the backscattering coefficient is converted *via* the simulated scattering phase function into the scattering coefficient. With this knowledge and extinction coefficient measured using a conventional photospectrometer, the absorption coefficient is calculated. We prove the validity of the method using spherical and rod-shaped gold nanoparticles, comparing the results with outputs from DDA simulations. We also briefly touch upon the dilemma of the choice of the appropriate dielectric function for gold at the nanoscale.

KEYWORDS: gold nanorods · plasmonic nanoparticles · differential pathlength spectroscopy · diffuse reflectance spectroscopy · backscattering coefficient · phase function · DDSCAT

Coherent surface plasmon oscillations due to the interaction of electromagnetic radiation with conduction-band electrons on the surfaces of noble metal nanoparticles result in an enhanced optical interaction with the nanoparticles at the resonance condition.[1] The spectral location of this plasmon resonance depends upon the interplay of wavelength, size, and shape of the particles. In the case of gold nanospheres, a single plasmon resonance-driven peak in absorption and scattering occurs at around 520 nm, which is responsible for the bright-red color of gold nanospheres.[1] In the case of core−shell particles, with a shell of gold on a silica core, hybridization of the plasmons from the outer and inner surfaces of gold causes splitting and shifting of the plasmon energies;[2] the low energy plasmon responsible for a red-shifted peak in the optical interaction. In the case of gold nanorods, symmetry breaking permits plasmon excitation along the two axes of the particle, the longitudinal plasmon results in a red-shifted optical interaction peak.[3]

Both core−shell and rod-shaped gold nanoparticles display an exquisite geometrical tunability of the location of the plasmon peak from the visible to the near-infrared (NIR) wavelengths.[2] The availability of these intense and narrow absorption/scattering peaks has generated enormous interest in applying these particles as photothermal therapeutic agents and as contrast agents for light-based imaging.[4−12]

In all biomedical applications, the enhanced contrast[13] or temperature effect is dependent on the concentration of the particles and their optical absorption coefficient (μ_{abs}) and/or scattering coefficient (μ_{sca}). Knowledge of these two parameters is therefore essential for making predictions of the efficacy of the particles.

Conventional optical spectroscopy in a UV−vis−NIR photospectrometer is a logical choice for determining optical properties but yields only the extinction coefficient (μ_{ext}). However, because $\mu_{ext} = \mu_{sca} + \mu_{abs}$, additional measurements are required to determine μ_{abs} and μ_{sca}. The conventional approach is to theoretically determine the extinction, absorption, and scattering cross sections (σ_{ext}, σ_{abs}, and σ_{sca}). When σ_{ext} is

*Address correspondence to a.amelink@erasmusmc.nl, s.manohar@tnw.utwente.nl.

Received for review November 27, 2009 and accepted June 07, 2010.

Published online June 17, 2010.
10.1021/nn1009165

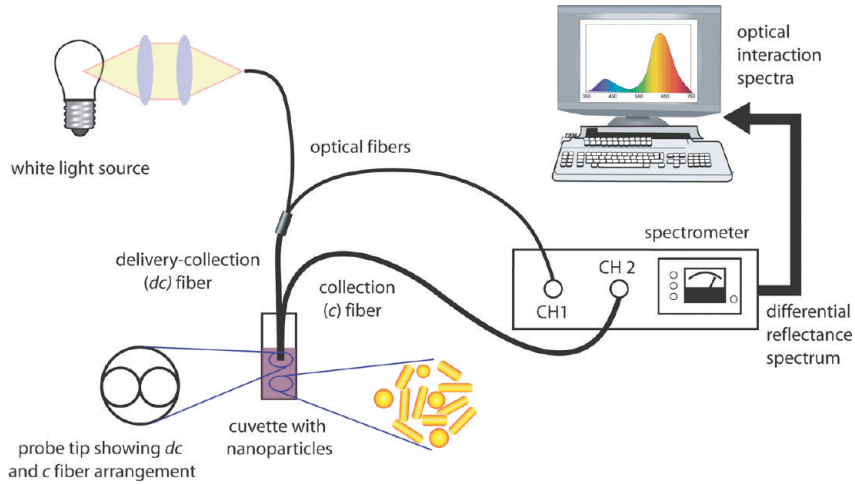

Figure 1. Differential pathlength spectroscopy experimental setup.

known, the concentration of the particles, *N*, can be calculated from the measured μ_{ext} as $N = \mu_{ext}/\sigma_{ext}$. This *N* with σ_{abs} and σ_{sca} is used to estimate μ_{abs} and μ_{sca}.

In order to theoretically determine σ_{ext}, σ_{abs}, and σ_{sca}, the sizes and shapes of the particles and their dielectric function are required. Average sizes are usually measured using electron microscopy (EM). Values of dielectric functions of the material (gold) and the embedding material (water) are usually obtained from the literature. With this knowledge, optical interaction efficiencies (Q_{ext}, Q_{abs}, and Q_{sca}) are calculated using Mie theory[1] (for spherical particles) or T-Matrix[14] and discrete dipole approximation (DDA) methods,[15] such as DDSCAT (for arbitrarily shaped particles). Again, from size data, the average geometrical cross sections are known, so that the interaction cross sections (σ_{ext}, σ_{abs}, σ_{abs}) can be calculated. This knowledge leads to determination of μ_{abs} and μ_{sca} *via N* as discussed above.

The drawbacks of the conventional method are primarily two-fold. While EM is indispensable for examination of individual particles, it samples low numbers of particles (250−300 particles) from lots comprising typically 10^{10} particles. This approach induces uncertainty in particle size estimation and affects the accuracy of Q_{ext} and σ_{ext} from DDA simulations. Further, we have shown that the choice of dielectric function affects the optical properties strongly.[16] There are two sources of dielectric function[17,18] that are usually used for simulating gold optical properties, and the data can be treated by size corrections when applied to nanoparticles. There is no universal agreement about which of these data give correct results, and one or other data set is used without justification or acknowledgment of the existence of other sources.

Currently, only a few experimental techniques have been reported against the backdrop of the limitations of the conventional approach. Approaches include the double integrating sphere method,[19] optical coherence tomography (OCT),[20,22] and recently a photoacoustic method.[23] The double integrating sphere method has the disadvantage of requiring careful sample alignment, possibility of nonlinear response of the spheres, and absorption of some diffuse photons by the sample precluding their detection.[21] OCT has the disadvantage of using a narrow emission bandwidth light source (Ti:sapphire laser[20]). Therefore, the measurements of the optical properties of gold nanoparticles can be determined only at a limited number of wavelengths. In methods which involve pulsed laser irradiation,[23] as in photoacoustic approaches, there exists the possibility of photothermal reshaping of the particles, which can affect the accuracy of the measurement.

We present here a novel approach to determine the ensemble optical properties of gold nanoparticles, more accurate, less expensive, and more economical with sample volumes than the ones reported in the literature. This method is based on a dual-fiber approach called differential pathlength spectroscopy (DPS),[24,25] developed originally for the early detection and diagnosis of cancer by localized endoscopic measurements of tissue optical properties. We extend its use to gold nanoparticles by measuring backscattering coefficients (μ_{bk}) of the particles in the single scattering regime.

DPS is based on reflectance measurements using two-fibers—one fiber delivers and collects (*dc*) photons from the sample; the second fiber adjacent to the first only collects (*c*) photons. When the scattering mean free path of photon is smaller than the fiber diameter, the differential reflectance, **R**, obtained by subtracting the *c* signal from the *dc* signal, has been shown to originate from a constant apparent pathlength. This term, called the differential pathlength,[24] depends only upon the fiber diameter, so that its knowledge allows quantitative determination of the optical properties in scattering media. A schematic of the experimental setup[25] is shown in Figure 1.

In the regime where the scattering mean free path of photons is greater than the fiber diameter, the differential signal cancels out multiple/single scattering events originating from deeper layers and is

responsive only to photons that have undergone single or a few scattering events[26] in a localized volume of a few hundred micrometers depth. When a fiber of small numerical aperture (say NA= 0.22) is used, the backscattering signal is given by[25]

$$\mathbf{R}_{sing} = C_{app}\mu_{bk} \quad (1)$$

where C_{app} is an instrumental constant (discussed later) and μ_{bk} the backscattering coefficient. This μ_{bk} can be thought as that fraction of the scattered photons that returns to the fiber. In other words

$$\mathbf{R}_{sing} = C_{app}\mathbf{p}(180)\mu_{sca} \quad (2)$$

where **p**(180) is the phase function of scattering sampled at 180°. Thus, from eq 2, it is clear that the acquired DPS signal can be related to μ_{sca}.

To convert this to the scattering coefficient (μ_{sca}), a theoretical calculation of the phase function at 180° of the particles **p**(180) is required. We use DDA simulation, but we show that this **p**(180) is only marginally susceptible to error, in sharp contrast to the simulated optical interaction efficiencies. Finally, using μ_{ext} from a standard UV−vis−NIR photospectrometer measurement, μ_{abs} is easily obtained.

RESULTS AND DISCUSSION

Determination of Calibration Constant. Figure 2 shows the theoretical backscattering coefficient, μ_{bk}, of the NIST-certified polystyrene beads of 51.4 and 95.6 nm diameter, calculated from DDSCAT and the chi square (χ^2) fitted DPS signal. The excellent fit between theoretical and measured spectra demonstrates that the measurements are in the single scattering regime. The fitting parameter yields inverse of C_{app} and was averaged for both sizes of beads for different concentrations between 10^9 and 10^{12} particles/mL. The variation in the calibration constant was <3% and acceptable for further use to scale all differential reflectance (**R**) spectra acquired from unknown samples to obtain μ_{bk} (see eq 1).

Calculation of p(180) for Gold Nanoparticles. The scattering phase function at 180° is obtained by simulation using DDSCAT. As mentioned earlier, the interaction efficiencies derived from the simulation are strongly affected by the input parameters such as size and dielectric function of the material chosen to depict the nanoparticle and can possess inaccuracies and uncertainties.[16] On the other hand, the value **p**(180) is hardly influenced by the chosen dielectric function, as depicted in Figure 3a for a gold nanosphere of diameter 40 nm and in Figure 3b for a gold nanorod of length 47.8 nm and diameter 23.3 nm. The sources of dielectric function of gold were from Johnson and Christy[17] and Palik,[18] with both bulk values and size corrected; the variation introduced in **p**(180) is less than 1% for spheres and less than 5% for gold nanorods.

We extended this study on **p**(180) dependence on different sources of dielectric function to other morphologies and sizes of particles. The results shown in the Supporting Information show that **p**(180) varies only marginally with dielectric function in each case.

Application on Samples under Investigation. ***Gold Spheres.*** Figure 4a displays μ_{ext} of 40 nm gold sol measured using the conventional photospectrometer and μ_{bk} derived from DPS experimental data using C_{app} and **p**(180). Figure 4b plots the μ_{sca} and μ_{abs}, leading from data in Figure 4a together with the parameters determined using the conventional method using dielectric functions from Palik.[18] It is clear that there is excellent agreement between the values, indicating the validity of the approach in determining μ_{sca} and μ_{abs}.

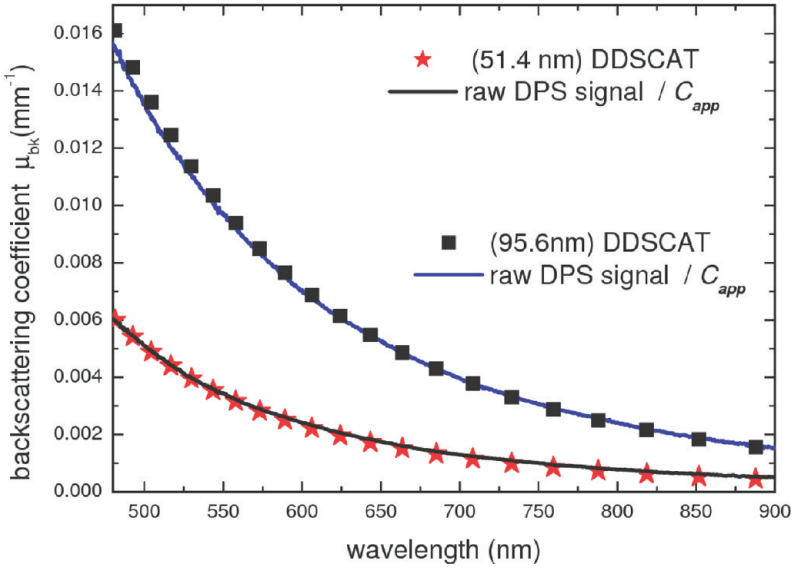

Figure 2. Backscattering coefficient of 51.4 and 95.4 nm beads calculated with DDSCAT (red stars and black squares, respectively) and corresponding raw DPS signal divided by the same C_{app}.

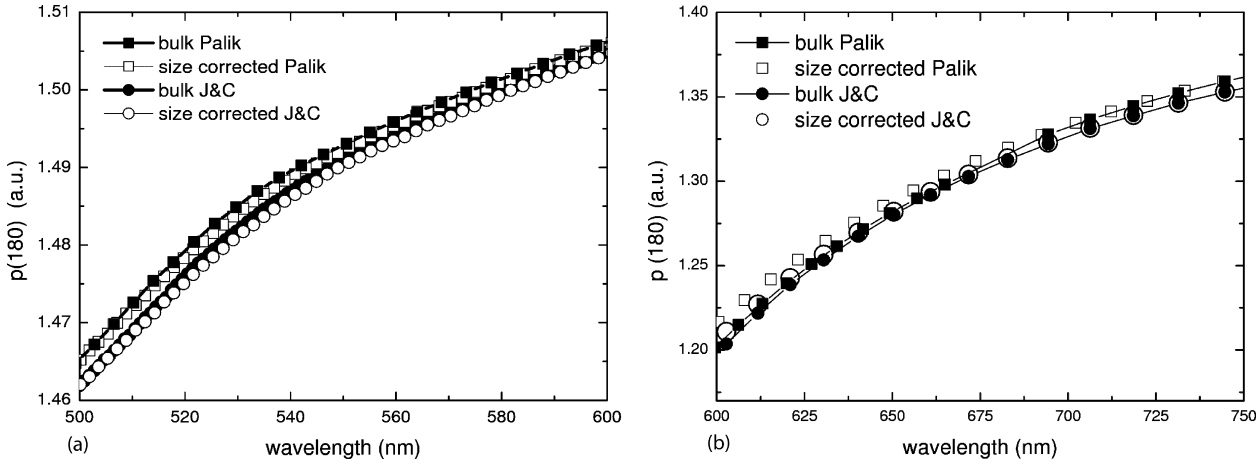

Figure 3. Influence of different sources of dielectric function on the simulation of phase function at 180° for (a) a gold nanosphere of diameter 40 nm, and (b) a gold nanorod of dimensions 47.8 nm × 23.3 nm.

We also observe that spectra obtained from the conventional method using dielectric function data from Palik,[18] instead of from Johnson and Christy,[17] provide the best agreement with values determined using the DPS method (Figure 5).

Gold Nanorods. The μ_{ext} and backscattering μ_{bk} spectra of gold nanorods $AuNR_{632}$ are shown in Figure 6a with the **p**(180) for particles calculated using the dielectric function from Palik.[18] From Figure 6a, we can observe that the transverse plasmon (TP) peak is pronounced in the μ_{ext} spectrum, and it is absent in the μ_{bk} spectrum. This suggests that the scattering cross section (ρ_{sca}) seen by light exciting transverse plasmons is negligibly small for these particles. The absorption cross section (σ_{abs}) is more emphatic, and this is manifested in the transverse plasmon band in the extinction spectrum, which has also been observed by Qiu *et al.*[27] in their scattering experiments on individual gold nanorods.

The derived μ_{sca} and μ_{abs} spectra are shown in Figure 6b. These have been calculated using **p**(180), simulated using DDSCAT for the two sources of dielectric function. The values for size-corrected dielectric functions are not shown because, as seen in Figure 3, the **p**(180) for size-corrected and bulk dielectric function is the same, which will translate in identical values of μ_{sca} and μ_{abs}. We see that the spectra in both cases overlap, confirming that the small dielectric function dependent variation in **p**(180) has negligible influence on the final results using the DPS approach.

However, a comparison of the DPS-derived spectra and those from the conventional method results in a poor match. This does not reflect on shortcomings in the DPS approach; rather it demonstrates the drawbacks discussed above, where the conventional method depends on the simulation of interaction efficiencies which are susceptible to errors.[16] This is less of an issue with nanospheres as we see above since, in general, the control over monodispersity of gold nanospheres is much tighter than in the case of gold nanorods. Further, the real and imaginary parts of the dielectric functions extracted from Palik,[18] on the one hand, and Johnson and Christy,[17] on the other, are close together in the range of 500−600 nm. Beyond this, the values begin to diverge, which introduces uncertainty in the choice of dielectric function for the simulations.

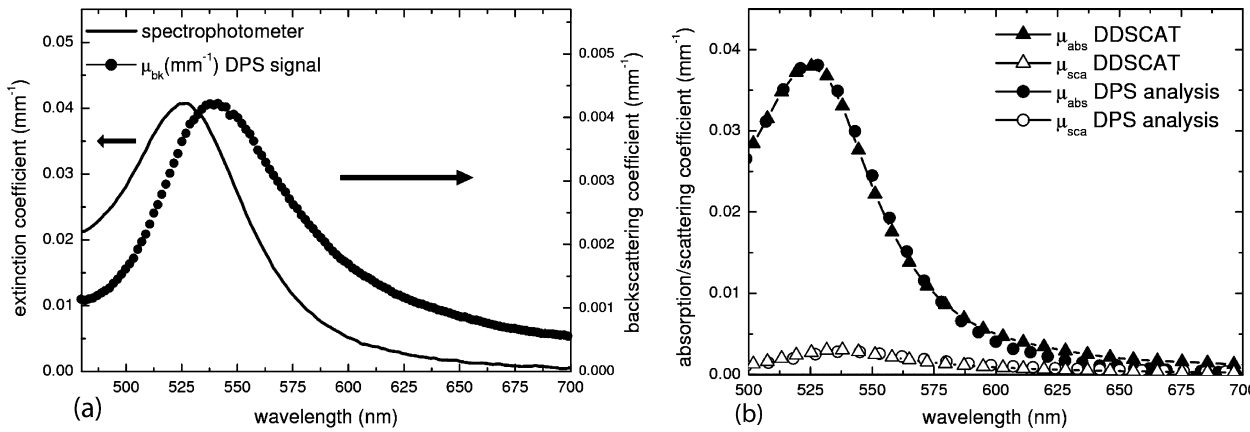

Figure 4. Backscattering coefficient as measured with DPS system and corresponding (a) extinction coefficient measured with the photospectrometer and (b) absorption and scattering coefficient determined using both conventional and DPS-based method for 40 nm gold spheres (bulk Palik[18] dielectric function).

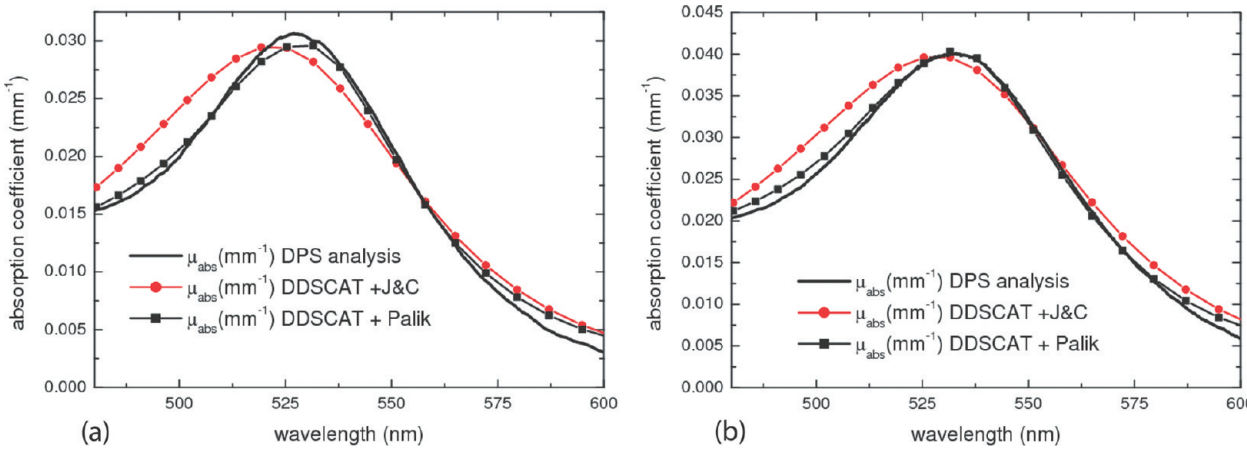

Figure 5. Absorption coefficient determined with DPS and calculated using conventional approach with bulk values of dielectric function from Johnson and Christy[17] and Palik[18] for (a) 50 nm and (b) 60 nm gold spheres, respectively

It can be argued that optical property estimation as outlined could be inaccurate since the method also depends on the calculation of **p**(180), which in turn depends on various parameters that could be inaccurately determined. To dispel this argument, we have studied the effect on **p**(180) of dielectric functions and size corrections in addition to the nanorods and nanospheres, also on nanocylinders and nanoshells. We show in Supporting Information that in all cases **p**(180) has a weak dependence on dielectric function variants within each shape and size case.

Further, we also investigated the behavior of **p**(180) for various sizes that could be encountered within a real sample. Figure 7 shows the distributions of lengths and widths in a histogram of size distributions in the lot of gold nanorods with the longitudinal plasmon peak at 632 nm. The average length × width is 47.8 × 23.3 nm. From the size distribution, we chose extreme values to set up two nanorods for simulation with sizes of 41 × 19 and 55 × 28 nm.

Figure 8a shows the **p**(180) values for these two particles. The differences are not greater than 5% at any wavelength. These values of **p**(180) are used with the DPS-derived backscatter coefficient to calculate the scatter coefficient and finally the absorption coefficient. Figure 2b shows the end result of μ_a against wavelength for the two **p**(180) values. The variations are marginal. The conclusion is that, for the ranges of polydispersity normally encountered in samples prepared, this method is not affected by the vagaries in dielectric function sources and leads to an accurate estimation of the optical properties.

A question is this: can the method be applied for samples that are unknown in shape, degree of inhomogeneity, and composition? Such samples do not fall in the gamut of particles that we wish to apply this technique for. We concentrate on characterizing nanoparticles that have been synthesized for use in nanomedicine applications. These particles owing to the very nature of the *in vivo* applications intended for them will not be unknown. These are the types of specimens that require optical characterization, and within the ranges of polydispersity (see Figure 7) typically reported for such samples, our technique is eminently suited for this task.

However, there is fundamentally no restriction in using the method on unknown samples if an additional measurement is performed. This is the measurement of

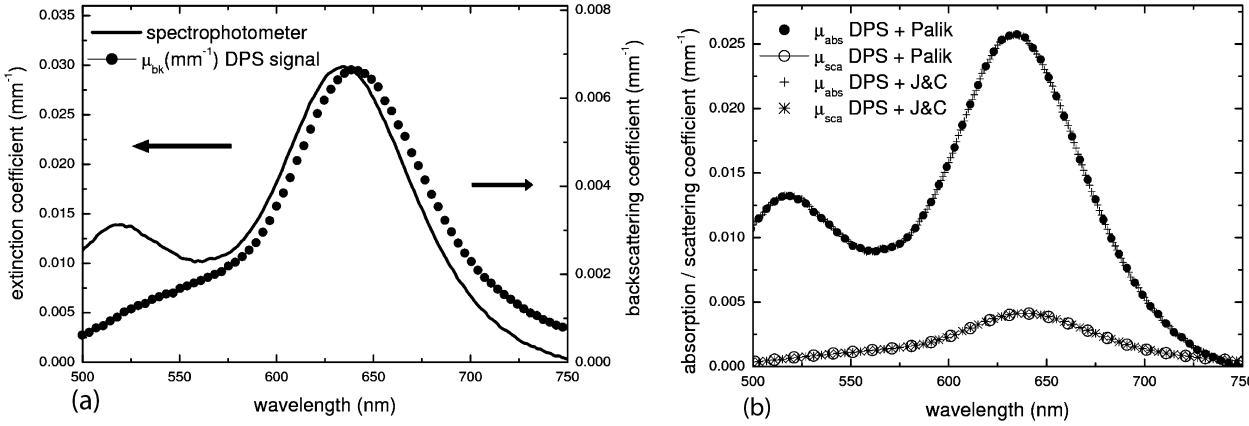

Figure 6. (a) Backscattering and extinction spectrum measured with DPS and conventional photospectroscopy and (b) absorption and scattering coefficient determined using the DPS method for AuNR$_{632}$ and with p(180) obtained using bulk dielectric function of Palik[18] and Johnson and Christy.[17]

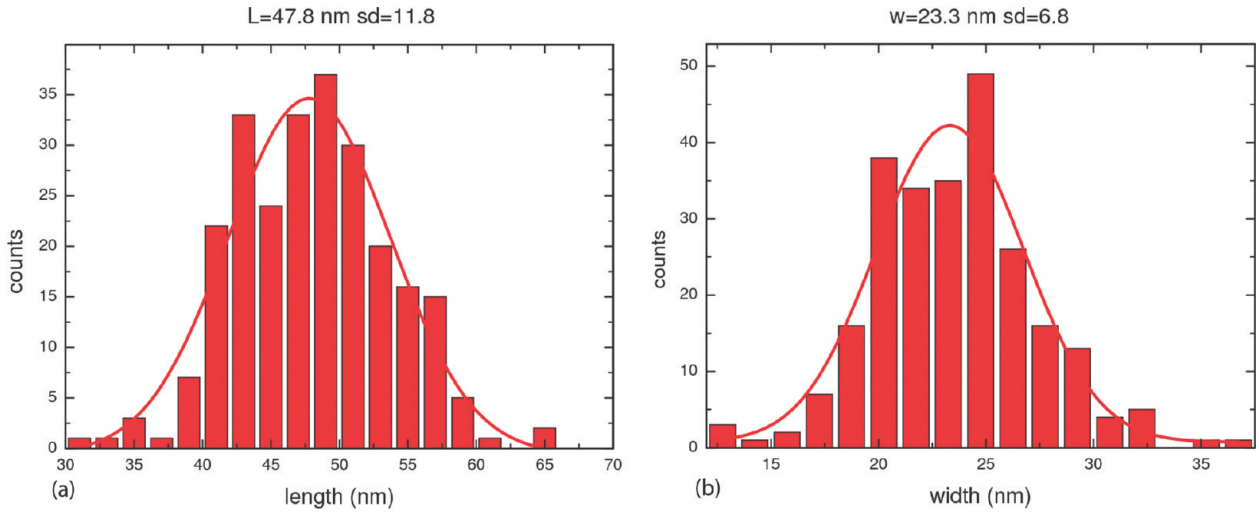

Figure 7. Measured size distribution for gold nanorods with a longitudinal plasmon (LP) peak at 632 nm.

the angular light scattering behavior which is possible using a goniometric approach. The measurement will allow the estimation of the average phase function of the particles, which when sampled at 180° can provide the required optical properties from the DPS-derived data.

Some caveats have to be kept in mind to attain high accuracies using our method. The calibration of the DPS system with the use of well-characterized media is of crucial importance. Uncertainties or errors in the inputs required for the correct optical description of the reference particles (size, refractive index of the particles, refractive index of the embedding medium, concentration of particles) will result in the extraction of an incorrect instrument constant. This error will propagate *via* subsequent calculation steps to the scattering and absorption coefficients. The use of NIST-certified polystyrene beads is recommended for avoiding these problems.

Further, the sample must be maintained at a concentration where single scattering dominates the differential reflectance signal—this is an important condition for eqs 1 and 2 to be applicable. This experimental condition, while guaranteeing accuracy, brings with it the advantageous consequence that low concentrations of particles can be used for gold nanoparticles typically 10^8 particles/mL. Verification of this condition can be done by monitoring the dependence of μ_{bk} on dilution; a linear dependence indicates that the single scattering regime is in dominance.

The estimation of μ_{abs} and μ_{sca} is important in characterizing particles for identifying or optimizing application such as photothermal therapy, photoacoustic imaging, and microscopies. Further, the measurement and analysis protocol calculates μ_{bk} in an early step, a parameter that allows calculation of the backscattering albedo $a' = \mu_{bk}/\mu_{ext}$, which may have relevance in OCT.[20]

As the application of plasmonic nanoparticles moves into the crucial phase of clinical trials, with the grant of approval from the U.S. FDA for human patient studies using gold nanoshells, the availability and use of these particles are set to explode in the near future. In this exciting period, where several fascinating methods[28] have been unveiled for the synthesis of the particles,

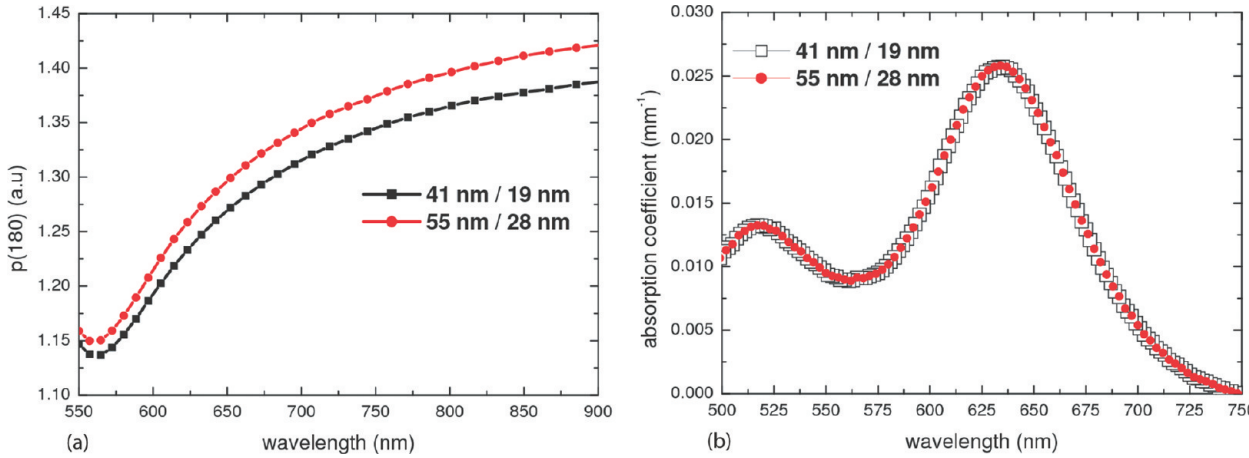

Figure 8. (a) Gold nanorod p(180) spectrum with dimensions of 55 × 28 nm and 41 × 19 nm. (b) Absorption coefficient spectrum for the same particles determined using DPS analysis using these p(180) spectra.

significantly the field is still lacking in the availability of methods to quickly characterize the particles. We believe that the DPS approach can fill the gap in the field of optical characterization of the nanoparticles. Further, the DPS system is predominantly used for the measurement of local optical properties of tissue, either intraoperatively or minimally invasive in the sense of an endoscopic measurement. The approach outlined here then provides a novel manner to extend the use of DPS to studying the loading of plasmonic particles in target areas in tissue. One could think of studying distribution of the nanoparticle-based molecular probes at a tumor site interoperatively to determine normal and diseased tissue and define tumor margins, which is crucial in tissue-sparing cancer surgery. Another application can be the detection or localization of sentinel nodes, when plasmonic nanoparticles and the DPS approach are used as the optical analogue of radiopharmaceuticals and γ-cameras in lymphoscintigraphy.

CONCLUSION

We show that differential pathlength spectroscopy (DPS) can be used to quantitate the ensemble optical properties of plasmonic nanoparticles. The differential reflectance signal from a nanoparticle sample in a well-calibrated DPS setup can be used to estimate the backscattering coefficient (μ_{bk}) under the condition of single scattering. With knowledge of the phase function of the nanoparticles at 180° obtained from simulations, the scattering coefficient (μ_{sca}) is calculated from the backscatter coefficient (μ_{bk}). The absorption coefficient (μ_{abs}) can then easily be derived from these two coefficients. The technique is accurate, quick, simple, and inexpensive. The analysis protocol is robust and less susceptible to errors and uncertainties that plague other conventional methods. Moreover, a wide absorption and scattering spectrum (400−900 nm) can be determined from a single measurement, limited only by the bandwidth of spectrophotometer and light source. Accurate knowledge of the optical properties of these nanoparticles serves as a means of characterizing them, which is important where the response to photothermal therapy requires one to be able to predict and to estimate contrast in photoacoustic imaging or in OCT. Additionally, we predict that this method will open up new applications in monitoring the presence of the nanoparticles in tissue at tumor sites.

MATERIAL AND METHODS

Differential Pathlength Spectroscopy. In the DPS device, light from a halogen light source (HL-2000-FHSA Ocean Optics, Duiven, The Netherlands) is coupled into one arm of a bifurcated fiber, which at its distal end is fed into the *dc* (delivery and collection) fiber. Reflected photons from the sample that are collected by the *dc* fiber travel through the second arm of the bifurcated fiber and into the first channel of the spectrophotometer (SD 2000 Ocean Optics, Duiven, The Netherlands). Reflected photons collected by the *c* (collection) fiber travel directly into the second channel of the spectrophotometer. Both *dc* and *c* collecting fibers are 400 μm in diameter and are arranged adjacent to each other within the probe and touching to minimize the distance between them. Specular reflections at the probe tip are minimized by polishing the fiber tips at an angle of 15°.

Nanoparticle samples were diluted in MilliQ water to get approximate scattering coefficients of the order of 10^{-2} mm^{-1}; the photon mean free path is greater than 100 mm and considerably larger than the fibers' diameter. Further, the NA of the fiber is arranged to be 0.22, maintaining a low acceptance angle, so that eq 2 can be applied. To minimize back reflections from the walls of the container, measurements are performed by inserting the probe into dispersions contained in black plastic cuvettes with volumes of 30 mL.

Polystyrene Beads. In order to determine the instrument constant C_{app} in eq 1, the DPS system requires calibration against media with well-characterized optical properties. We used NIST-certified polystyrene beads (Polysciences Inc., Warrington, PA) for this purpose. The particles were 51.4 ± 7.3 nm in diameter (particle concentration 1.01% w/v) and 95.6 ± 4.9 nm in diameter (particle concentration 1% w/v).

Gold Nanospheres and Gold Nanorods. Validation of the DPS-based method was performed using gold spheres with diameters of 40, 50, and 60 nm (British Biocell International, UK). Gold nanorods with their longitudinal plasmon (LP) peak at 632 nm (referred to as $AuNR_{632}$) were also studied. These particles were synthesized in our laboratory using a seed-mediated surfactant and silver-assisted growth protocol.[29]

In this protocol derived from Nikoobakht and El-Sayed,[30] growing cetyltrimethylammonium bromide (CTAB)-capped gold nanospheres are used to seed a growth solution comprising gold salt (primed with a mild reducing agent ascorbic acid), the surfactant CTAB, and silver nitrate ($AgNO_3$). Addition of seed initiates the reduction of elemental gold preferentially on certain facets of the gold seed, resulting in the formation of nanorods. By changing the volume of $AgNO_3$ added in the reaction, the aspect ratios of the nanorods can be tuned.[29]

Information about the size and shape of gold nanoparticles used was retrieved from analysis of digital images obtained using high-resolution scanning electron microscopy (HR-SEM). The analysis was performed on approximately 250 particles. Extinction spectra were measured using a photospectrometer (UV−vis−NIR 3101PC, Shimadzu Deutschland GmbH, Duisburg, Germany). A HR-SEM picture of gold nanorods used in this experiment is shown in Figure 9.

Optical Properties Simulation. Optical properties of the particles used for DPS analysis were simulated using the DDSCAT 6.1 software.[15] This code is a popular implementation of the DDA method originally developed by Purcell and Pennypacker.[31] The numerical method divides the analyzed particle in dipoles, and the electric field radiated by the particles is calculated taking into account interaction between all of these dipoles. The main advantage of this approach is that, in principle, any shape can be generated and simulated.

The polystyrene beads were simulated with inputs from the manufacturer's data sheets and with a refractive index calculated using the relation $1.5607 + 10002/\lambda^2$, where λ is the wavelength in nanometers.[32]

For the gold particles, dielectric functions were used from both Johnson and Christy[17] and Palik.[18] There is as yet no universal agreement about the choice between the two sources, and we decided to investigate the influence of choosing one or another on the results. We studied both the bulk values and size-corrected values.[16] Water with refractive index of 1.33 was chosen as a medium in which the nanoparticles were dispersed.

Measurement and Analysis Protocol. The following steps are followed:

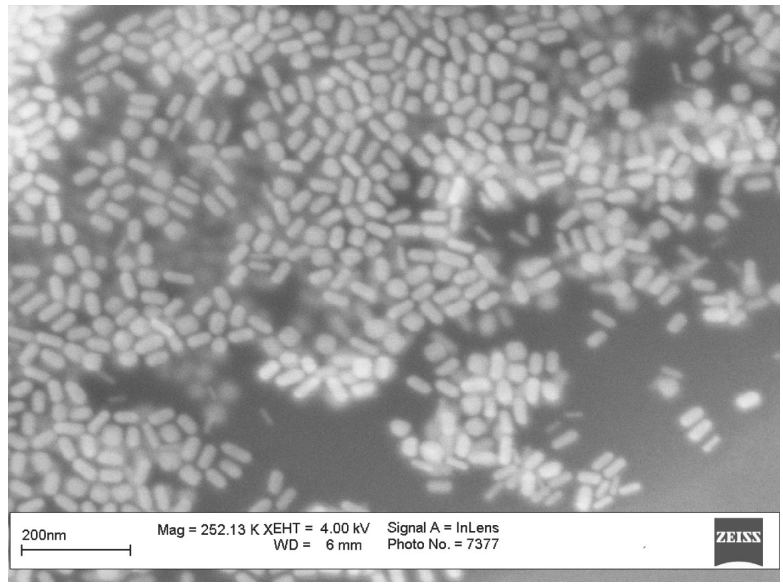

Figure 9. High-resolution scanning electron microscope (HR-SEM) image of gold nanorods with a longitudinal plasmon (LP) peak at 632 nm. The particles are on average 47.8 nm long and 23.3 nm wide.

Determine the Instrument Constant C_{app}. To account for lamp and detector spectral features, measurements are performed at both *dc* and *c* fibers (*I* and *J* outputs, respectively), with a diffuse white reflectance standard (I_{white} and J_{white}) and diffuse black reflectance standard (I_{black} and J_{black}).

Then a reference measurement (I_n) is done with *dc* fiber in a fluid with appropriate refractive index matching the sample to correct for reflections that occur at the probe−sample interface and those from the container walls which may occur despite using a large black container. The differential reflectance signal is then given by

$$\mathbf{R} = k\left[\frac{I - I_n}{I_{white} - I_{black}} - \frac{J}{J_{white} - J_{black}}\right] \quad (3)$$

$$\equiv k(I_{dc} - J_c) \quad (4)$$

In the above, *k* is a constant that is dependent on the distance between the probe tip and the reference samples. Further, in order to apply eq 2 to unknown samples, differential reflectance signal (**R**) must be scaled by the inverse of the C_{app} to yield the backscatter coefficient (μ_{bk}). This instrument constant can then be defined as the proportionality constant, which translates the experimentally measured **R** into the quantitative sample parameter μ_{bk} and depends among others upon *k* above.

To determine C_{app}, the system is calibrated against the NIST certified polystyrene beads in the following way:

- Using DDSCAT code, the backscattering efficiency (Q_{bk}) is calculated for the polystyrene beads using the inputs from manufacturer's data sheets.
- DPS signals are then recorded for various dilution of the beads. By comparing the spectra of **R** and Q_{bk}, the range of dilutions for which single scattering is the principal contributor to the differential reflectance signal is determined. For concentrations of the beads above the upper limit, multiple scattering events are recorded in dominance, which deteriorates **R** in comparison with Q_{bk}; for very low concentrations the signal-to-noise ratio is low.
- The theoretical backscattering coefficient (μ_{bk}) for the beads is calculated as:

$$\mu_{bk} = N_p \pi r^2 Q_{bk} \quad (5)$$

where N_p is the number of particles calculated from the data sheets and dilution ratios, *r* is the radius of the polystyrene beads, and Q_{bk} is the backscattering efficiency calculated earlier.

- The instrument constant C_{app} is now determined as the average scaling factor that allows the best fit of **R** to the μ_{bk} using a least-squares optimization or chi-square (χ^2) fitting method.

Measure the DPS Signal from the Unknown Sample and Recover the Backscattering Coefficient. The probe is inserted into the cuvette, and **R** spectra are recorded. The data are then scaled by the inverse of the instrument constant C_{app} to convert them into an equivalent backscattering coefficient spectrum.

Estimate the Phase Function and Recover the Scattering and Absorption Coefficients. From HR-SEM, the average size and shape of the gold nanorods are ascertained. The scattering phase function is calculated for the range of wavelengths of interest using DDSCAT. Scattering coefficient is determined further using eq 2 and **p**(180) calculated at this point. Finally, scattering coefficient is subtracted from μ_{ext} measured using the photospectrometer to yield μ_{abs}.

Acknowledgment. This work is funded through the thrust area program NIMTIK of the University of Twente, through the PRESMITT project (IPD067771) of the SenterNovem program IOP Photonic Devices, and by the Nederlandse Wetenschappelijk Organisatie (NWO) and Stichting Technische Wetenschappen (STW) through Project TTF 6527.

Supporting Information Available: Additional figures and experimental details. This material is available free of charge *via* the Internet at http://pubs.acs.org.

REFERENCES AND NOTES

1. Bohren, C. Huffman, D. *Absorption and Scattering of Light by Small Particles*; Cambridge University Press: New York, 1998.
2. Prodan, E.; Radloff, C.; Halas, N. J.; Nordlander, P. A Hybridization Model for the Plasmon Response of Complex Nanostructures. *Science* **2003**, *302*, 419–422.
3. Link, S.; El-Sayed, M. Size and Temperature Dependence of the Plasmon Absorption of Colloidal Gold Nanoparticles. *J. Phys. Chem. B* **1999**, *103*, 4212–4217.
4. El-Sayed, I.; Huang, X.; El-Sayed, M. Selective Laser Photothermal Therapy of Epithelial Carcinoma Using Anti-egfr Antibody Conjugated Gold Nanoparticles. *Cancer Lett.* **2006**, *239*, 129–135.
5. Hirsch, L. R.; Stafford, R. J.; Bankson, J. A.; Sershen, S. R.; Rivera, B.; Price, R. E.; Hazle, J. D.; Halas, N. J.; West, J. L. Nanoshell-Mediated Near-Infrared Thermal Therapy of Tumors under Magnetic Resonance Guidance. *Proc. Natl. Acad. Sci. U.S.A.* **2003**, *100*, 13549–13554.

6. O'Neal, D. P.; Hirsch, L. R.; Halas, N. J.; Payne, J. D.; West, J. L. Photo-thermal Tumor Ablation in Mice Using Near Infrared-Absorbing Nanoparticles. *Cancer Lett.* **2004**, *209*, 171–176.
7. Dickerson, E. B.; Dreaden, E. C.; Huang, X.; El-Sayed, I.; Chu, H.; Pushpanketh, S.; McDonald, J. F.; El-Sayed, M. Gold Nanorod Assisted Near-Infrared Plasmonic Photothermal Therapy (PPTT) of Squamous Cell Carcinoma in Mice. *J. Am. Chem. Soc.* **2008**, *269*, 57–66.
8. Eghtedari, M.; Oraevsky, A. A.; Copland, J. A.; Kotov, N. A.; Conjusteau, A.; Motamedi, M. High Sensitivity of *In Vivo* Detection of Gold Nanorods Using a Laser Optoacoustic Imaging System. *Nano Lett.* **2007**, *7*, 1914–1918.
9. Mallidi, S.; Larson, T.; Tam, J.; Joshi, P. P.; Karpiouk, A.; Sokolov, K.; Emelianov, S. Multiwavelength Photoacoustic Imaging and Plasmon Resonance Coupling of Gold Nanoparticles for Selective Detection of Cancer. *Nano Lett.* **2009**, *9*, 2825–2831.
10. Li, P.-C.; Wang, C.-R. C.; Shieh, D.-B.; Wei, C.-W.; Liao, C.-K.; Poe, C.; Jhan, S.; Ding, A.-A.; Wu, Y.-N. *In Vivo* Photoacoustic Molecular Imaging with Simultaneous Multiple Selective Targeting Using Antibody-Conjugated Gold Nanorods. *Opt. Express* **2008**, *16*, 18605–18615.
11. Wang, Y.; Xie, X.; Wang, X.; Ku, G.; Gill, K. L.; O'Neal, D. P.; Stoica, G.; Wang, L. V. Photoacoustic Tomography of a Nanoshell Contrast Agent in the *In Vivo* Rat Brain. *Nano Lett.* **2004**, *4*, 1689–1692.
12. Yang, X.; Skrabalak, S. E.; Li, Z.-Y.; Xia, Y.; Wang, L. V. Photoacoustic Tomography of a Rat Cerebral Cortex *In Vivo* with Au Nanocages as an Optical Contrast Agent. *Nano Lett.* **2007**, *7*, 3798–3802.
13. Faber, D.; van Velthoven, M.; de Bruin, M.; Aalders, M.; Verbraak, F.; Graf, C.; van Leeuwen, T. Naomi: Nanoparticles Assisted Optical Molecular Imaging. *Proc. SPIE.* **2006**, *6079*, 607905.
14. Mishchenko, M. I.; Travis, L. D.; Mackowski, D. W. T-Matrix Computations of Light Scattering by Nonspherical Particles: A Review. *J. Quant. Spectrosc. Radiat. Transfer* **1996**, *55*, 535–575.
15. Draine, B. T.; Flatau, P. J. *User Guide to the Discrete Dipole Approximation Code DDSCAT 6.1*, http://arxiv.org/abs/astro-ph/0409262v2.
16. Ungureanu, C.; Rayavarapu, R. G.; Manohar, S.; van Leeuwen, T. G. Discrete Dipole Approximation Simulations of Gold Nanorod Optical Properties: Choice of Input Parameters and Comparison with Experiment. *J. Appl. Phys.* **2009**, *105*, 102032.
17. Johnson, P. B.; Christy, R. W. Optical Constants of the Noble Metals. *Phys. Rev. B* **1972**, *6*, 4370–4379.
18. Palik. E. D., Ed. *Handbook of Optical Constants of Solids*; Academic Press: New York, 1991.
19. Oldenburg, A. L.; Zweifel, D. A.; Xu, C.; Wei, A.; Boppart, S. A. Characterization of Plasmon-Resonant Gold Nanorods as Near-Infrared Optical Contrast Agents Investigated Using a Double-Integrating Sphere System. *Proc. SPIE* **2005**, *5703*, 50–60.
20. Oldenburg, A. L.; Hansen, M. N.; Zweifel, D. A.; Wei, A.; Boppart, S. A. Plasmon-Resonant Gold Nanorods as Low Backscattering Albedo Contrast Agents for Optical Coherence Tomography. *Opt. Express* **2006**, *14*, 6724–6738.
21. Welch, A. J., van Gemert, M. J. C., Eds. *Optical-Response of Laser-Irradiated Tissue (Lasers, Photonics, and Electro-Optics)*; Plenum Press: New York, 1995.
22. Cang, H.; Sun, T.; Li, Z.-Y.; Chen, J.; Wiley, B. J.; Xia, Y.; Li, X. Gold Nanocages as Contrast Agents for Spectroscopic Optical Coherence Tomography. *Opt. Lett.* **2005**, *30*, 3048–3050.
23. Cho, E. C.; Kim, C.; Zhou, F.; Cobley, C. M.; Song, K. H.; Chen, J.; Li, Z.-Y.; Wang, L. V.; Xia, Y. Measuring the Optical Absorption Cross Sections of Au−Ag Nanocages and Au Nanorods by Photoacoustic Imaging. *J. Phys. Chem. C* **2009**, *113*, 9023–9028.
24. Amelink, A.; Bard, M. P. L.; Burgers, S. A.; Sterenborg, H. J. C. M. Single-Scattering Spectroscopy for the Endoscopic Analysis of Particle Size in Superficial Layers of Turbid Media. *Appl. Opt.* **2003**, *42*, 4095–4101.
25. Amelink, A.; Sterenborg, H. J. C. M. Measurement of the Local Optical Properties of Turbid Media by Differential Path-Length Spectroscopy. *Appl. Opt.* **2004**, *43*, 3048–3054.
26. van de Hulst, H. C. *Light Scattering by Small Particles*; Dover Publications Inc.: New York, 1981.
27. Qiu, L.; Larson, T. A.; Smith, D. K.; Vitkin, E.; Zhang, S.; Modell, M. D.; Itzkan, I.; Hanlon, E. B.; Korgel, B. A.; Sokolov, K. V.; Perelman, L. T. Single Gold Nanorod Detection Using Confocal Light Absorption and Scattering Spectroscopy. *IEEE J. Sel. Top. Quantum Electron* **2007**, *13*, 1730–1738.
28. Xia, Y.; Xiong, Y.; Lim, B.; Skrabalak, S. E. Metal Nanocrystals: Simple Chemistry Meets Complex Physics. *Angew. Chem.* **2009**, *48*, 60–103.
29. Rayavarapu, R. G.; Petersen, W.; Ungureanu, C.; Post, J.; van Leeuwen, T. G.; Manohar, S. Synthesis and Bioconjugation of Gold Nanoparticles as Potential Molecular Probes for Light-Based Imaging Techniques. *Int. J. Biomed. Imaging* **2007**, 29817.
30. Nikoobakht, B.; El-Sayed, M. A. Preparation and Growth Mechanism of Gold Nanorods (NRs) Using Seed-Mediated Growth Method. *Chem. Mater.* **2003**, *15*, 1957–1962.
31. Purcell, E. M.; Pennypacker, C. R. Scattering and Absorption of Light by Nonspherical Dielectric Grains. *Astrophys. J.* **1973**, *186*, 705–714.
32. Marx, E.; Mulholland, G. W. Size and Refractive Index Determination of Single Polystyrene Spheres. *J. Res. Natl. Bur. Stand.* **1983**, *88*, 321–338.